

Photoacoustic characterization of chalcogenide glasses: Thermal diffusivity of $\text{Ge}_x\text{Te}_{1-x}$

J. C. de Lima, N. Cella, and L. C. M. Miranda*

Instituto Politécnico do Rio de Janeiro, Caixa Postal 97282, 28613, Nova Friburgo, Rio de Janeiro, Brazil

C. Chying An, A. H. Franzan, and N. F. Leite

Laboratório Associado de Sensores e Materiais, Instituto de Pesquisas Espaciais, Caixa Postal 515, 12201, São José dos Campos, São Paulo, Brazil

(Received 25 March 1992)

The photoacoustic technique is used to investigate the thermal diffusivity of $\text{Ge}_x\text{Te}_{1-x}$ glasses as a function of composition. The observed dependence on the composition is explained on the basis of the chemically ordered network model. This interpretation is further supported by x-ray and electrical resistivity measurements.

INTRODUCTION

The continuing interest in the last two decades on the investigation of the chalcogenide glasses reflects not only the interesting scientific questions posed by these materials but also their use as switching and memory devices.¹ Intensive experimental investigations on $\text{A}^{\text{IV}}\text{B}^{\text{VI}}$ glasses reveal that physical properties like refractive index, coefficient of thermal expansion, optical band gap, dielectric constant, electrical resistivity, Raman scattering, etc., exhibit an anomalous (sudden) change at the $x=0.2$ and 0.33 compositions.²⁻⁷ In the $\text{Ge}_x\text{Te}_{1-x}$ glassy system, the optical band gap,⁸ as well as the thermal crystallization,⁹ exhibit marked changes in their behavior at the $x=0.2$ composition, whereas acoustic attenuation studies¹⁰ in $\text{Ge}_x\text{S}_{1-x}$ and $\text{Ge}_x\text{Se}_{1-x}$ show peaks in attenuation at $x=0.2$ and 0.33 . In contrast, except for a few papers^{11,12} on glassy $\text{As}_x\text{Te}_{1-x}$ and $\text{Ge}_x\text{Se}_{1-x}$, respectively, there seems to exist no systematic investigation of the thermal diffusivity of chalcogenide glasses in the literature.

The thermal diffusivity α , defined as $\alpha = k/\rho c$, where k is the thermal conductivity, ρ the mass density and c the specific heat, is an important physical parameter to be monitored not only by its intrinsic physical interest but also for its use in device modeling and design. Physically, the inverse of α is a measure of the time required to establish thermal equilibrium in a given material. Like the optical-absorption coefficient, it is unique for each material. This can be appreciated from the tabulated values of α given by Touloukian *et al.*¹³ for a wide range of materials, such as metals, minerals, foodstuffs, and biological specimens. Furthermore, the thermal diffusivity is also known to be extremely dependent upon the effects of compositional and microstructural variables¹⁴ as well as processing conditions as in case of polymers,¹⁵⁻¹⁹ ceramic,¹⁴ and glasses.²⁰

The photoacoustic (PA) effect²¹ has been proved by several authors²²⁻²⁶ to be a simple and reliable technique for measuring the thermal properties of solid samples. The PA effect looks directly at the heat generated in a

sample, due to nonradiative deexcitation processes, following the absorption of light. In the conventional experimental arrangement, a sample is enclosed in an airtight cell and exposed to a chopped light beam. As a result of the periodic heating of the sample, the pressure in the cell oscillates at the chopping frequency and can be detected by a sensitive microphone coupled to the cell. The resulting signal depends not only on the amount of heat generated in the sample (and, hence, on the optical absorption coefficient and the light-into-heat conversion efficiency of the sample) but also on how the heat diffuses through the sample determined by the thermal diffusivity. In this paper, we apply the recently proposed open-photoacoustic cell (OPC) configuration^{27,28} for investigating the effects of the composition on the thermal diffusivity of $\text{Ge}_x\text{Te}_{1-x}$.

EXPERIMENT

The $\text{Ge}_x\text{Te}_{1-x}$ samples of different compositions were prepared by the conventional melt quenching technique. Appropriate amounts of 5N pure germanium and tellurium were introduced in a quartz ampoule (8-mm inner diameter), evacuated to 10^{-6} Torr and sealed. The ampoule was then kept in a furnace at a temperature of 820°C and was periodically rotated to ensure good homogeneous mixing of the melt. After 24 h the ampoule were rapidly quenched and the samples were then taken out. The amorphous nature of the samples was checked by x-ray diffraction. The measurements were carried out with a Philips powder goniometer using the $\text{Cu K}\alpha$ radiation. In Fig. 1 we show the x-ray diffractogram for the $x=0.20$ composition, which, indeed, corresponds to that of an amorphous solid. The OPC experimental arrangement is schematically shown in Fig. 2. It consists of using a 150-W halogen-tungsten lamp whose polychromatic beam, after being heat filtered, is mechanically chopped and focused onto the sample. The sample is mounted directly onto a circular electret microphone. The typical design of a electret microphone^{29,30} consists of a metalized electret diaphragm [12- μm FEP (hexafluoro-

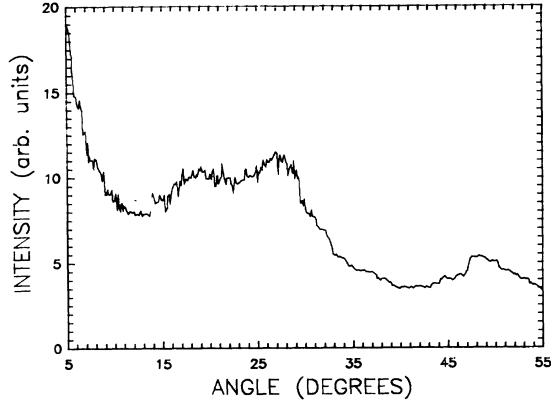


FIG. 1. X-ray diffractograms for $\text{Ge}_x\text{Te}_{1-x}$ samples for compositions $x = 0.20$ showing amorphous structure.

propylene-tetrafluoroethylene copolymer) with a 500–1000-Å-thick deposited-metal electrode] and a metal backplate separated from the diaphragm by an air gap (45 μm long).

The metal layer and the backplate are connected through a resistor R . The front sound inlet is a circular hole of 3-mm diameter, and the front air chamber adjacent to the metalized face of the diaphragm is roughly 1 mm long. As a result of the periodic heating of the sample by the absorption of modulated light, the pressure in the front chamber oscillates at the chopping frequency, causing diaphragm deflections, which generates a voltage across the resistor. This output voltage from the microphone is connected to a lock-in amplifier in which the signal amplitude and phase are both recorded as a function of the modulation frequency. The use of a heat-filter for the light beam ensured us that we were just focusing the visible part of the spectrum onto the sample, in which range the samples are all optically opaque. This means that we can safely assume that the heat is deposited essentially at the sample front surface. Under these conditions, the pressure fluctuation in the air chamber is given by^{27,28}

$$\delta p = \frac{P_0 I_0 (\alpha_g \alpha_s)^{1/2}}{2\pi l_g T_0 k_s f \sinh(l_s \sigma_s)} e^{j(\omega t - \pi/2)}, \quad (1)$$

where $P_0(T_0)$ is the ambient pressure (temperature), I_0 is

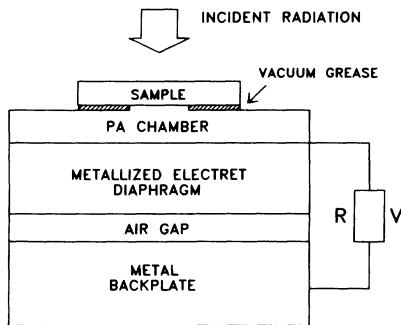


FIG. 2. Cross section of the open-photoacoustic cell using the front air chamber of a common electret microphone as a transducer medium.

the incident light intensity, f is the modulation frequency, and l_i , k_i and α_i are the length, thermal conductivity, and thermal diffusivity of material i . Here, the subscript i denotes the sample (s) and gas (g) media, respectively, and $\sigma_i = (1+j)a_i$, with $a_i = (\pi f / \alpha_i)^{1/2}$ being the thermal diffusion coefficient of material i .

For sufficiently thin samples, such that, $l_s a_s \ll 1$, Eq. (1) reduces to

$$\delta p \cong \frac{P_0 I_0 \alpha_g^{1/2} \alpha_s}{(2\pi)^{3/2} T_0 l_g k_s l_s} \frac{e^{j(\omega t - 3\pi/4)}}{f^{3/2}}. \quad (2)$$

In other words, the PA signal amplitude decreases as $f^{-1.5}$ as one increases the modulation frequency. In contrast, for thicker samples, such that $l_s a_s \gg 1$, Eq. (1) gives us

$$\delta p \cong \frac{P_0 I_0 \alpha_g \alpha_s}{\pi T_0 l_g k_s l_s} \frac{\exp[-l_s (\pi f / \alpha_s)^{1/2}]}{f} \times \exp[j(\omega t - \pi/2 - l_s a_s)]. \quad (3)$$

Equation (3) means that, for a thermally thick sample, the amplitude of the PA signal decreases exponentially with the modulation frequency as $(1/f)\exp(-a\sqrt{f})$, where $a = (\pi l_s^2 / \alpha_s)^{1/2}$. The thermal diffusivity α_s can then be obtained from the signal amplitude data, as a function of the modulation frequency, by fitting it to the expression

$$S = (A/f) \exp(-a\sqrt{f}). \quad (4)$$

Knowing, the coefficient a from the fitting procedure, α_s is readily obtained from

$$\alpha_s = \pi (l_s / a)^2.$$

In Fig. 3 we show the PA signal amplitude as a function of the frequency square root for the 220- μm -thick $x = 0.2$ sample. The solid curve in this figure represents

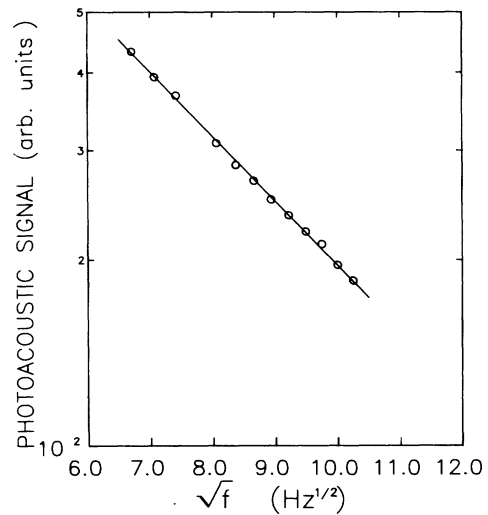


FIG. 3. Open-photoacoustic cell signal amplitude as a function of the modulation frequency square root for a 220- μm -thick sample with $x = 0.20$. The solid curve represents the data fitting to Eq. (4) of the text.

the fitting of the experimental data to Eq. (4). The resulting value of α from the data fitting was $\alpha=0.027\pm 0.002$ cm^2/s for the $x=0.2$ sample. For the tellurium sample ($x=0.0$) the value we got for α was $\alpha=0.013\pm 0.002$ cm^2/s . The literature value¹³ for crystalline Te is 0.02 cm^2/s . The same procedure was repeated for the other alloy compositions. In Fig. 4 we summarize the results for the thermal diffusivity as a function of the composition parameter x for our $\text{Ge}_x\text{Te}_{1-x}$ samples. The solid curve in Fig. 4 represents the data interpolation to a polynomial expression so that the peak could be more precisely identified. The thermal diffusivity exhibited two peaks, one at the $x=0.20$ composition and another one at $x=0.5$. The peak at the $x=0.20$ composition can be explained by the chemically ordered network model³¹⁻³⁴ for chalcogenide glasses. According to this model, for the $A\text{-Te}$ ($A=\text{Ge}, \text{Si}$) system in the glass forming region, namely, $x < 0.33$, the system contains both $A\text{-Te}$ and Te-Te bonds, and for $x > 0.33$ both $A\text{-Te}$ and $A\text{-A}$ bonds are present. At low concentrations of A atoms the glass system is characterized essentially by one-dimensional Te chains. As the concentration of A atoms increases, the Te chains are increasingly cross linked by A atoms, thus changing the one-dimensional chain into a three-dimensional network at $x=0.20$. It is said that at this composition a percolation transition^{32,33} from a polymeric glass to a rigid amorphous solid takes place. The jump at $x=0.20$ reflects this percolation transition threshold to the formation of a rigid amorphous solid offering minimum resistance to the heat propagation. The second peak in Fig. 4 at $x=0.5$ corresponds to the formation of GeTe solid solution. In fact, the phase diagram of Ge-Te systems^{35,36} shows that GeTe is formed at $x=0.5$ by a peritectic reaction at 725 °C.

Next, and to further support these findings, we have measured the electrical resistivity of our samples as a function of the composition as a shown in Fig. 5. The data in Fig. 5 exhibit one sharp peak at $x=0.20$ and a second smaller and broader peak at $x=0.30$. These maxima in the electrical resistivity are consistent with the

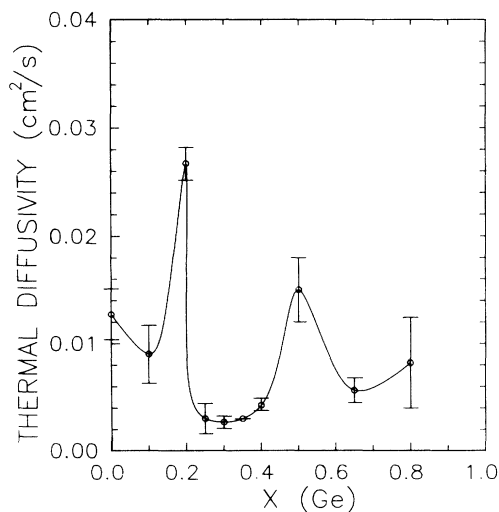


FIG. 4. Thermal diffusivity of $\text{Ge}_x\text{Te}_{1-x}$ as a function of composition.

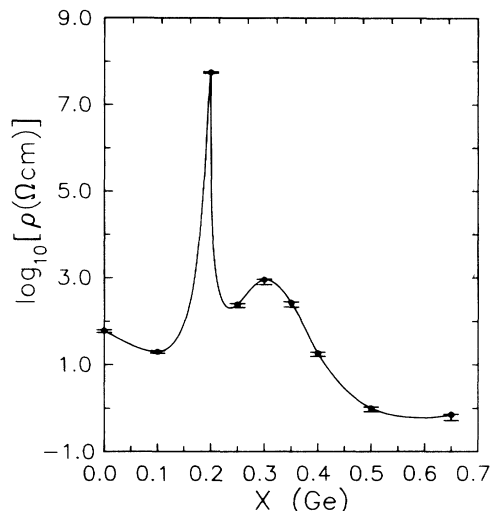


FIG. 5. Electrical resistivity (\log_{10}) of $\text{Ge}_x\text{Te}_{1-x}$ as a function of composition measured at room temperature.

maximum density of stable structural units as suggested by Feltz and Pfaff.³⁶ The peak at $x=0.20$ is associated with the formation of the rigid amorphous solid, whereas the peak at $x=0.30$ is more readily interpreted on the basis of new network structures of the type proposed in Refs.^{36,37} Feltz and Pfaff³⁶ proposed that $\text{Ge}(\text{Se}_2)_2$ structural units are present in $\text{Ge}_x\text{Se}_{1-x}$ glasses. In the present case, ditelluride bonds would be present at $x=0.30$ giving rise to stable structural units like  with the reduction in the number of unsatisfied bonds.³⁶ This reduction of unsatisfied bonds leads to a maximum in the resistivity.

DISCUSSION AND CONCLUSIONS

In this paper we have reported on the behavior of the thermal diffusivity and the electrical resistivity of $\text{Ge}_x\text{Te}_{1-x}$ alloys as a function of composition. The thermal diffusivity exhibited two peaks one at $x=0.2$ and another one at $x=0.5$, whereas the peaks in the electrical resistivity were centered at the $x=0.2$ and 0.3 compositions. According to the chemically ordered network model, the glass-forming tendency is maximized at the critical average coordination number $\langle m_c \rangle = 2.4$. At this point a perfect network is formed such the number of force field constraints exhausts the number of degrees of freedom. The average coordination number for the $\text{Ge}_x\text{Te}_{1-x}$ system is given by

$$\langle m \rangle = xN_{\text{Ge}} + (1-x)N_{\text{Te}}, \quad (5)$$

where N_{Ge} and N_{Te} are the Ge and Te coordination numbers, respectively. In the glass-forming region, namely, $x < 0.33$, $N_{\text{Ge}}=4$ and $N_{\text{Te}}=2$,³⁶ so that the critical composition x_c leading to the formation of a perfect network is $x=0.20$. Glasses with $x < x_c$ are inadequately constrained and tends to disintegrate into nonpolymerized fragments; i.e., the glasses contain rigid and floppy regions with the floppy regions dominating. Increasing x ,

the rigid regions increase in volume until, at $x = x_c$, a percolation transition takes place to a rigid network of the compound composition GeTe_2 . Disorder in the network is minimum at this composition and it increases as we move away from x_c . This explains the observed sharp peaks at $x = 0.20$ in both α and the electrical resistivity. Away from the glass-forming region the system behaves as a random mixture two-phase system consisting of GeTe and excess Te or Ge atoms depending whether x is smaller or greater than $x = 0.5$, respectively. At $x = 0.5$, only GeTe is formed and the thermal diffusivity exhibits a second peak corresponding to a more organized state.

These results for the thermal diffusivity of $\text{Ge}_x\text{Te}_{1-x}$ glasses agree with those for $\text{As}_x\text{Te}_{1-x}$ but differ from the ones reported for $\text{Ge}_x\text{Se}_{1-x}$ glasses. For $\text{As}_x\text{Te}_{1-x}$, Madhusoodanan *et al.*¹¹ found a single peak at $x = 0.4$, which corresponds to an average coordination number $\langle m \rangle = 2.4$ for this system. This is equivalent, in our case, to the peak at $x = 0.2$. For $\text{Ge}_x\text{Se}_{1-x}$ glasses,¹² the thermal diffusivity exhibited two peaks in the glass-forming region; one at the $x = 0.2$ composition, corresponding to the threshold for the formation of a stable structure, and a second one at the stoichiometric composition $x = 0.33$. In our case, in the glass-forming region,

the thermal diffusivity showed a single peak at $x = 0.2$ corresponding to the formation of a fully polymerized rigid amorphous solid. The other peak, corresponding to the germanium monotelluride formation, occurred outside the glass-forming region at $x = 0.5$. These results indicate that the compositional dependence of the thermal diffusivity of chalcogenide glasses should be further investigated.

The electrical resistivity of our samples, on the other hand, apart from showing the strong and sharp peak at $x = 0.2$, it also exhibited a much smaller (roughly, five orders of magnitude) and broader peak at the $x = 0.3$ composition. The peak at the critical composition $x = 0.2$ agrees with the observations of Asokan, Parthasarathy, and Gopal⁵ for the electrical resistivity of $\text{Si}_x\text{Te}_{1-x}$ glasses. The second and smaller peak at $x = 0.3$ suggests the formation of new stable structural units as proposed by Feltz and Pfaff. This would correspond to the presence of ditelluride bonds leading to the formation of stable tetrahedral units of the type shown in the previous section. These structures, associated with the reduction of unsatisfied bonds in the $0.2 < x < 0.33$ region, were not sufficiently intense to manifest themselves in the thermal diffusivity data.

*On leave of absence from the Instituto de Pesquisas Espaciais, São José dos Campos, SP, Brazil.

¹D. Adler, *Sci. Am.* **236**, 36 (1977).

²R. Azoulay, H. Thibierge, and A. Brenac, *J. Non-Cryst. Solids*, **18**, 33 (1975).

³R. Ota, Y. Yamate, N. Soga, and M. Kunugi, *J. Non-Cryst. Solids* **29**, 67 (1978).

⁴R. J. Namanich, G. A. N. Connel, T. M. Hayes, and R. A. Street, *Phys. Rev. B* **18**, 6900 (1978).

⁵S. Asokan, G. Parthasarathy, and E. S. R. Gopal, *Phys. Rev. B* **35**, 8269 (1987).

⁶A. Feltz, H. Aust, and A. Blayer, *J. Non-Cryst. Solids* **55**, 179 (1983).

⁷P. Tronc, M. Bensoussan, and A. Brenac, *Phys. Rev. B* **8**, 5947 (1973).

⁸A. Deneuille, J. P. Keradec, P. Gerard, and A. Mini, *Solid State Commun.* **14**, 341 (1974).

⁹J. Cornet, *Ann. Chim. (Paris)* **10**, 239 (1979).

¹⁰K. S. Gilroy and W. A. Phillips, *Philos. Mag. B* **47**, 655 (1983).

¹¹K. N. Madhusoodanan, J. Philip, S. Asokan, and E. S. R. Gopal, *J. Mater. Sci. Lett.* **7**, 1333 (1988).

¹²K. N. Madhusoodanan and J. Philip, *Phys. Status. Solidi A* **108**, 775 (1988).

¹³Y. S. Touloukian, R. W. Powell, C. Y. Ho, and M. C. Nicolasu, in *Thermal Diffusivity* (IFI/Plenum, New York, 1973).

¹⁴G. Ziegler and D. P. H. Hasselman, *J. Mater. Sci.* **16**, 495 (1981).

¹⁵N. F. Leite, N. Cella, H. Vargas, and L. C. M. Miranda, *J. Appl. Phys.* **61**, 3023 (1987).

¹⁶A. Torres-Filho, L. F. Perondi, and L. C. M. Miranda, *J. Appl. Polym. Sci.* **35**, 103 (1988).

¹⁷B. Merté, P. Korpium, E. Lüscher, and R. Tilgner, *J. Phys. (Paris) Colloq.* **44**, 463 (1983).

¹⁸A. Torres-Filho, N. F. Leite, L. C. M. Miranda, N. Cella, and

H. Vargas, *J. Appl. Phys.* **66**, 97 (1989).

¹⁹A. H. Franzen, N. F. Leite, and L. C. M. Miranda, *Appl. Phys. A* **50**, 431 (1990).

²⁰A. C. Bento, H. Vargas, M. M. F. Aguiar, and L. C. M. Miranda, *Phys. Chem. Glasses* **28**, 127 (1987).

²¹H. Vargas and L. C. M. Miranda, *Phys. Rep.* **161**, 43 (1988).

²²M. J. Adams and G. F. Kirkbright, *Analyst* **102**, 281 (1977).

²³R. T. Swimm, *Appl. Phys. Lett.* **42**, 955 (1983).

²⁴C. L. Cesar, H. Vargas, J. Mendes-Filho, and L. C. M. Miranda, *Appl. Phys. Lett.* **43**, 555 (1983).

²⁵A. Lachaine and P. Poulet, *Appl. Phys. Lett.* **45**, 953 (1984).

²⁶O. Pessoa, Jr., C. L. Cesar, N. A. Patel, H. Vargas, C. C. Ghizoni, and L. C. M. Miranda, *J. Appl. Phys.* **59**, 1316 (1986).

²⁷M. S. Silva, I. N. Bandeira, and L. C. M. Miranda, *J. Phys. E* **20**, 1476 (1987).

²⁸L. F. Perondi and L. C. M. Miranda, *J. Appl. Phys.* **62**, 2955 (1987).

²⁹G. M. Sessler and J. E. West, in *Electrets*, Springer Series on Topics in Applied Physics, Vol. 33, edited by G. M. Sessler (Springer, Berlin, 1980), p. 347.

³⁰G. Lucovsky and T. M. Hayes, in *Amorphous Semiconductors*, edited by M. H. Brodsky (Springer, Berlin, 1979), p. 215.

³¹M. F. Thorpe, *J. Non-Cryst. Solids* **57**, 350 (1983).

³²J. C. Phillips and M. F. Thorpe, *Solid State Commun.* **53**, 699 (1985).

³³J. C. Phillips, *Phys. Rev. B* **31**, 8157 (1985).

³⁴N. K. Abrikosov, V. F. Bankina, L. V. Poretskaya, L. E. Shelimova, and E. V. Skudnova, in *Semiconducting II-VI, IV-VI and V-VI Compounds* (Plenum, New York, 1969), p. 67.

³⁵J. C. Phillips, *J. Non-Cryst. Solids* **34**, 153 (1979).

³⁶A. Feltz and G. Pfaff, *J. Non-Cryst. Solids* **77**, 1137 (1985).

³⁷W. Zhou, M. Paesler, and D. E. Sayers, *Phys. Rev. B* **43**, 2315 (1991).